

## CHARACTERISTICS OF THE pVINIS ION SOURCE

P. Beličev and D. Ćirić

*Vinča Institute of Nuclear Sciences, P. O. Box 522, 11001 Belgrade, Yugoslavia*

The pVINIS Ion Source is the light ion source of the TESLA Accelerator Installation. Basically, it is an injector consisting of two ion source bodies, and an analysing magnet. The sources are of the volume type with the multicusp magnetic field for plasma confinement. The injector is capable of delivering  $H^+$ ,  $H_2^+$ ,  $H_3^+$ ,  $D^+$ ,  $D_2^+$  and  $D_3^+$ , as well as  $H^-$  and  $D^-$  ions with maximal energy of 30 keV. The measured results of the ion beam emittance, profile and current, in the energy range from 8 to 30 keV are presented. The results obtained show very good ion beam quality, with the emittances smaller than  $50 \pi \text{ mm mrad}$ , as well as considerable currents, about 1 mA, meeting most of the requirements for cyclotrons with external ion sources.

### 1 Introduction

The TESLA Accelerator Installation comprises three main machines: an isochronous cyclotron - VINCY, an ECR ion source - mVINIS, and a multicusp ion source - pVINIS [1]. The pVINIS Ion Source is a light ion source capable of producing relatively intensive beams of both positive and negative hydrogen and deuterium ions. This source has been designed and produced by AEA Technology plc, Culham, UK. It will be primarily used for radioactive isotope production thus requiring routine, maintenance free operation for up to several days. It will be also applied during the cyclotron commissioning phase to produce beams with relatively low Q/A values (molecular ions  $D_2^+$  and  $D_3^+$ ).

### 2 Required Beam Parameters

The required beam parameters are determined by the operating range of the VINCY Cyclotron and by the main purpose of the light ion source pVINIS - radioactive isotope production. Different hydrogen ion species are needed to match the variety of the VINCY acceleration modes. The intention is to use  $H_2^+$ ,  $H_3^+$ , and  $D^-$  ions for isotope production, while  $H^+$  ions will be mainly used for research programs in order to avoid significant radioactive contamination of the accelerator components.  $D_2^+$  and  $D_3^+$  ions will be used only during the cyclotron commissioning. To minimize the time required for isotope production the demand is that the extracted current of  $H_2^+$ ,  $H_3^+$ , and  $D^-$  should be at least 500  $\mu\text{A}$  at maximum extraction voltage. The maximum extracted current of  $H^+$  should be restricted to 200  $\mu\text{A}$  for reasons described earlier.

Table 1: Required beam parameters of the pVINIS ion source

Ion	$V_{\text{ex}}$ [kV]	$I_{\text{ex}}$ [ $\mu\text{A}$ ]	$\epsilon_{\text{max}}$ (90%) [ $\pi \text{ mm mrad}$ ]
$H^-$	24 - 30	$\leq 200$	0.4
$D^-$	18 - 25	$\geq 500$	0.26
$H_2^+$	18 - 25	$\geq 500$	0.26
$H_3^+$	12 - 18	$\geq 500$	0.18
$D_2^+$	8 - 12	$\geq 200$	0.15
$D_3^+$	6 - 8	$\geq 200$	0.10

The required beam parameters (extraction voltage range, maximum extracted current and maximal  $\beta\gamma$ -normalized emittance) of different ion species from the pVINIS Ion Source are summarized in Table 1.

### 3 Ion Source Description

Basically, the pVINIS is an ion beam injector whose major parts are: ion source body, extraction/acceleration system, beam diagnostic system, analyzing magnet, vacuum system, power supplies and control system.

#### 3.1 Ion Source Body

The ion source is a bucket multicusp ion source with filament discharge. The magnetic field configuration is determined by the purpose of the source. Negative ion source is optimized for negative ion production. This configuration is not optimal for positive molecular ion production, particularly for  $H_2^+$  and  $D_2^+$ . Thus, the pVINIS Ion Source has two source bodies, one for positive and one for negative ion operation (changeover from one to another configuration is possible within 1-2 hours without venting the system). A schematic drawing of the source body, together with the extraction/acceleration system is shown in Fig. 1.

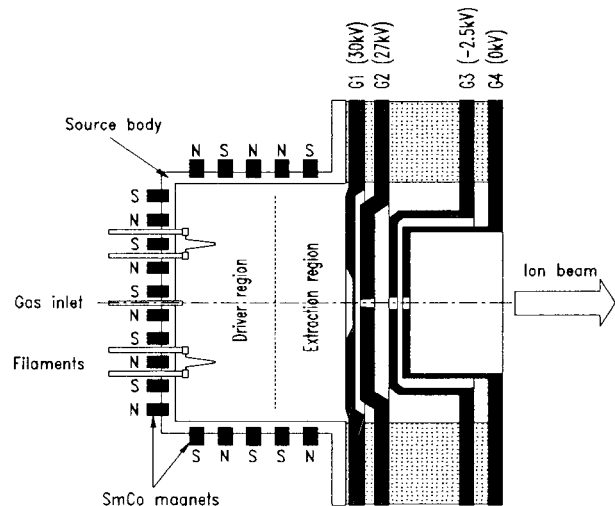


Fig. 1: Schematic drawing of the pVINIS Ion Source body.

The magnets surrounding the source from all sides except from the extraction plane side, form a high-order multipole field (so called multicusp configuration) which confines the plasma. Detailed magnetic field configuration depends on the purpose of the source. For negative ion sources, the magnet pattern is anti-symmetric, thus creating a transverse (dipole) magnetic field, which acts as a magnetic filter. This filter modifies the electron energy distribution inside the source and divides it into two regions: driver region and extraction region.

Each source body contains three hairpin lanthanum filaments, two of which working simultaneously, maintain the plasma discharge. In case of filament breakdown, it is possible to switch to the third filament in a matter of minutes.

The mechanism of the negative ion formation in this type of ion sources is explained in details elsewhere (e.g. [2]).

### 3.2 Extraction/Acceleration System

The extraction/acceleration system provides both the required ion beam energy and quality in terms of maximal beam dimension and divergence.

In the configuration for positive ions, as it is shown in Fig. 1, this system consists of four electrodes, designated from G1 to G4. Biasing G1 together with the ion source body to potential up to 30 kV, the energy of the ions is regulated. The G2 electrode focuses the beam matching it to the acceptance of the analysing magnet. The potential of this electrode can be varied up to 5 kV below the one of the G1. Applying negative potential up to -2.5 kV on the G3 electrode, the secondary electrons produced in the beam line downstream the source, are prevented from back-streaming. The G4 electrode is at ground potential.

The extraction/acceleration system in the negative ion configuration consists of three electrodes, having the same function as G1, G2 and G4 in the positive ion configuration. These electrodes are biased to reverse polarity with respect to those in the positive ion configuration. The problem of elimination of the co-extracted electrons is solved by installing two electron traps: a) the first one, near the aperture of the G1, consisting of small electrodes biased to slightly positive potential with respect to G1 (few volts), and b) the second one, by installing permanent dipole magnet at G2.

### 3.3 Beam Diagnostic and Analysing System

The system consists of a movable beam profile monitor of the Faraday cup type with a  $36 \times 0.5 \text{ mm}^2$  slit, a beam current monitor of the Faraday cup type, and an analysing magnet. The beam profile monitor, mounted on a diagnostic chamber 50 mm from the last extraction electrode of the source, is capable of measuring the beam current distribution in the vertical plane. Due to its position, it measures the unanalysed beam containing all ion species (e.g.  $\text{H}^+$ ,  $\text{H}_2^+$  and  $\text{H}_3^+$ ).

The beam current monitor is mounted after the analysing magnet and measures the current of a single ion species. The analysis of the ion beam is carried out by means of an air cooled,  $90^\circ$  stigmatic focusing analysing magnet, with 300 mm bending radius and 20 mm air gap. Maximal magnetic induction between the poles is 0.112 T.

### 3.4 Vacuum System

The necessary vacuum for operation of about  $10^{-7}$  mbar is achieved with two turbo-molecular vacuum pumps. The first one of 1000 l/s, situated before, and the second one of 300 l/s, situated after the analysing magnet. Two mechanical pumps of 18  $\text{m}^3/\text{h}$  and 12  $\text{m}^3/\text{h}$  provide the roughing and backing pressure. The level of the vacuum in the system is measured by three thermocouple and one cold cathode gauges.

### 3.5 Control System

Two operational modes of the pVINIS are possible: local and remote. In the local mode of operation, the control is achieved through a fiber optic data link system including transmitters and receivers for power supplies at high voltages. The remote control is based on Honeywell's Alcont 3000<sup>x</sup> industrial control system.

## 4 Measured Beam Parameters

The measurements of the beam parameters have been performed in two phases: a) at AEA Technology premises, after the two source bodies were fabricated [3], and b) at the Vinča Institute of Nuclear Sciences, during the commissioning of the pVINIS.

### 4.1 Ion Species Ratio Measurements

The ratio of the hydrogen ion species  $\text{H}^+$ ,  $\text{H}_2^+$  and  $\text{H}_3^+$  as well as of the deuterium ion species  $\text{D}^+$ ,  $\text{D}_2^+$  and  $\text{D}_3^+$ , were measured as a function of gas flow rate [3]. Fig. 2 shows the hydrogen species ratio as a function of gas flow rate, for the extracted total beam current of 4 mA. The analogue diagram for deuterium, for an extracted total beam current

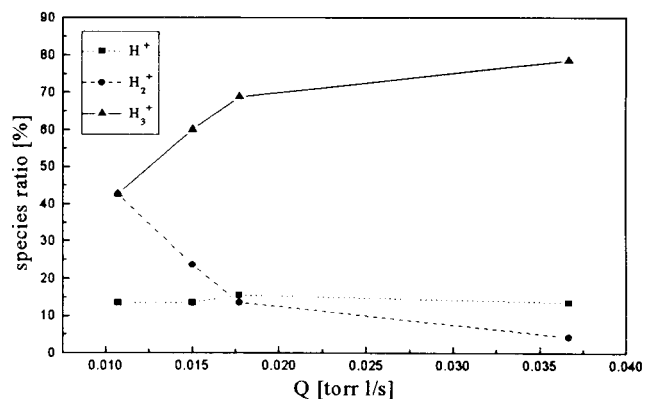


Fig. 2: Hydrogen species ratio vs. gas flow ratio.

of 3.7 mA, is shown in Fig. 3. The results show that  $H_2^+$  and  $D_2^+$  species become major component in the extracted total beam current for low values of the gas flow rate. It was found that for deuterium, maximising the  $D_2^+$  species concentration required much lower gas flow rates than for the hydrogen. Since the source cannot adequately operate at pressures much below 1 mbar, nitrogen was added in order to maintain the necessary pressure. The concentration of  $H_3^+$  and  $D_3^+$  rises with the gas flow rate.

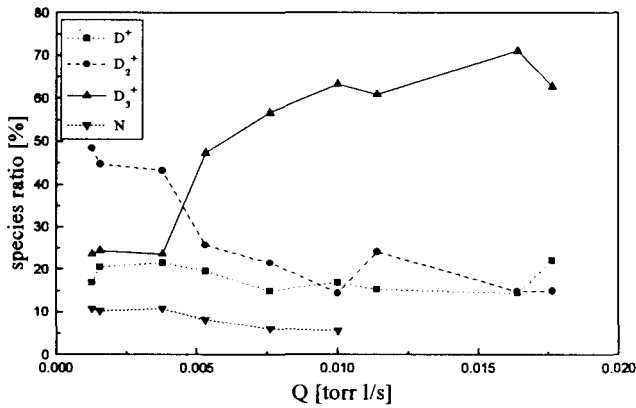


Fig. 3: Deuterium species ratio vs. gas flow ratio.

#### 4.2 Beam Emittance Measurements

The emittance measurements have been done using the two-slit method [4]. The emittance of the positive hydrogen ion beam (containing all species) was measured at the energy of 12 keV with gas flow rate of 0.037 torr l/s ( $H_3^+$  maximised) and at 25 keV with gas flow rate of 0.011 torr l/s ( $H_2^+$  maximised). The emittance diagram at 12 keV is shown in Fig. 4 as an example. The emittance fractional plot vs. beam fraction at 12 keV and 25 keV is given in Fig. 5. The emittance fractional plot vs. beam fraction for 8 keV positive deuterium ion beam, for two gas flow rates is given in Fig. 6.

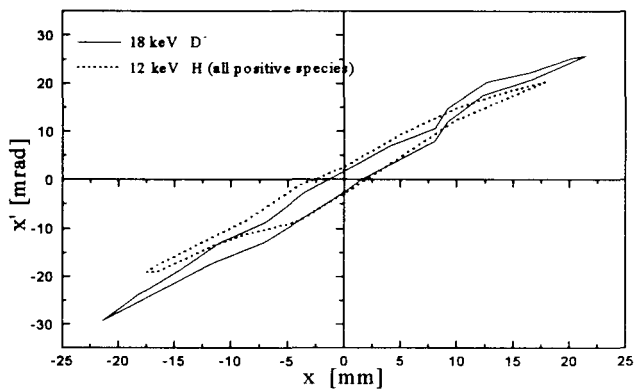


Fig. 4: Emittance diagrams of hydrogen and deuterium ion beams.

Note that there is considerable emittance growth when operating at low gas flows, probably due to reduced level of space neutralisation associated with a low background pressure [3].

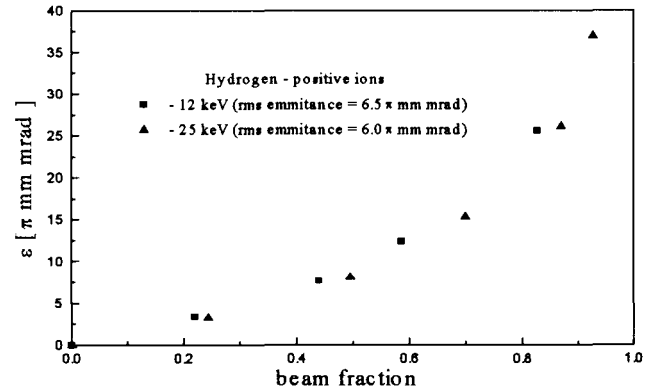


Fig. 5: Un-normalised emittance vs. beam fraction.

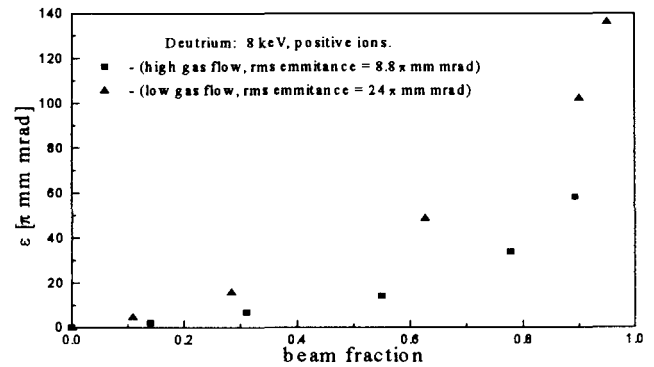


Fig. 6: Un-normalised emittance vs. beam fraction.

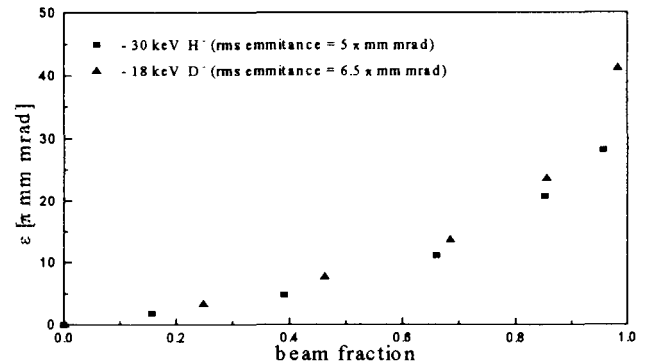


Fig. 7: Un-normalised emittance vs. beam fraction.

The emittance of the  $H^-$  and  $D^-$  beams were measured in the same way as for the positive ones, at energies of 30 keV and 18 keV respectively. The emittance diagram of  $D^-$  beam is shown in Fig. 4 as an example. The fractional plots for the two ion beams are shown in Fig. 7.

Table 2 : Measured beam parameters of the pVINIS Ion Source

Ion Species	E [keV]	$I_{total}$ [mA]	Gas Flow [torr l/s]	$\epsilon_n$ (90%) [ $\pi$ mm mrad]
$H^-$	30	3.3	0.04	0.18
$H_2^+$	25	7.8	0.011	0.16
$H_3^+$	12	2.6	0.04	0.13
$D^-$	18	1.2	0.04	0.13
$D_2^+$	12	2.0	0.015	0.13
$D_3^+$	8	1.6	0.04	0.11

The values of  $\beta\gamma$ -normalised emittances, containing 90% of the beam particles, for all ion species, are given in Table 2.

#### 4.3 Beam Current and Profile Measurements

The measurements of the beam current distribution were performed in the vertical plane only, assuming axial symmetry of the beam immediately after its extraction. Typical beam profiles for positive and negative hydrogen ion beams at 20 keV are depicted in Fig. 8 and Fig. 9, showing twice wider positive than negative profile.

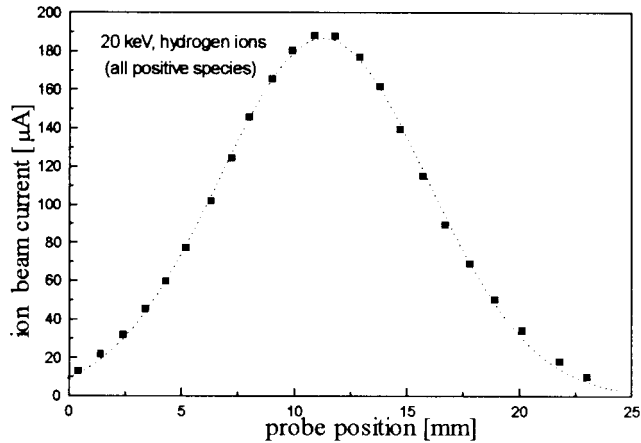


Fig. 8 Beam current distribution.

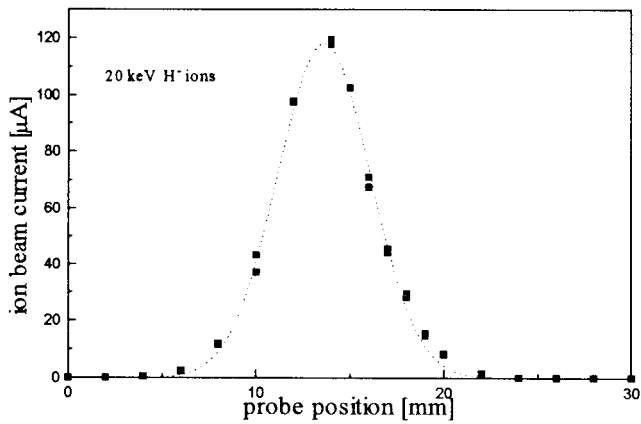


Fig. 9: Beam current distribution.

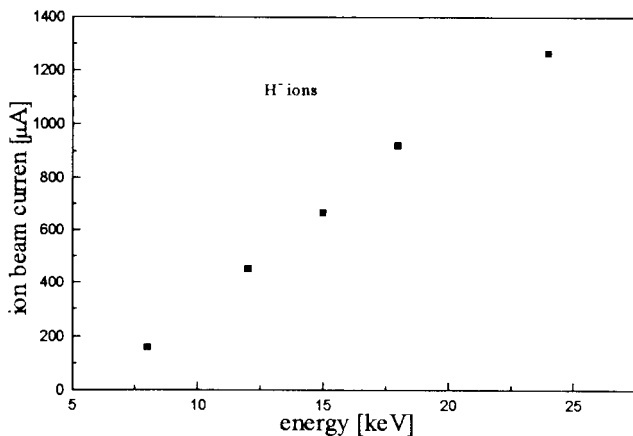


Fig. 10: Maximal  $H^-$  beam current vs. ion energy.

Figures 10 and 11 show the maximal extracted currents of  $H_2^+$ ,  $H_3^+$  and  $H^-$  ion beams as a function of the ion energy. Considering the values for the total extracted currents from Table 2 as well as the species ratio in Fig. 2, it is obvious that it should be possible to extract even higher currents than the obtained ones. Having in mind that the beam diameter from Fig. 8 ( $\sim 20\text{mm}$ ) is close to the analysing magnet's air gap, it seems that the main beam losses are due to its collision against the magnet's vacuum chamber. Increasing the magnet's air gap (which will cause higher electric power consumption and introducing water cooling) it will be possible to get significantly higher beam currents. Having in mind that the required beam parameters from Table 1 are met even with the low acceptance (but simple and low consumption) analysing magnet, the losses of the beam can be tolerated.

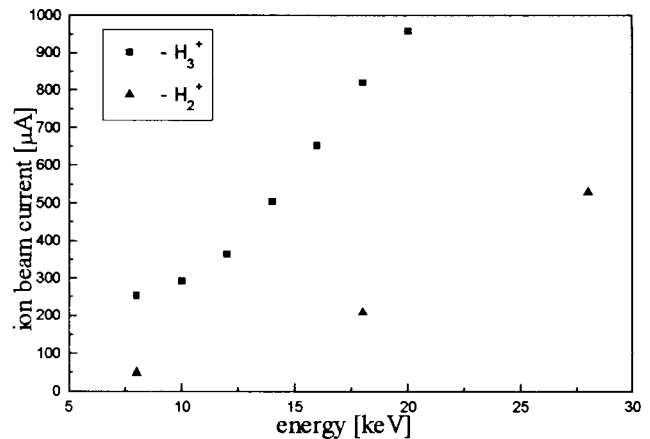


Fig. 11: Maximal  $H_2^+$  and  $H_3^+$  beam current vs. ion energy.

#### 5 Conclusion

The pVINIS Ion Source is capable of delivering  $H^+$ ,  $H_2^+$ ,  $H_3^+$ ,  $D^+$ ,  $D_2^+$  and  $D_3^+$ , as well as  $H^-$  and  $D^-$  ions with maximal energy of 30 keV. The results obtained show very good ion beam quality, with the emittances smaller than  $50 \pi \text{ mm mrad}$ , as well as considerable currents, about 1 mA, meeting most of the requirements for cyclotrons with external ion sources.

#### References

- [1] N. Nešković et al., *Proceedings of the 14th International Conference Cyclotrons and their Applications*, Cape Town, October 8-13, 1995 (World Scientific, Singapore, 1995), p. 82.
- [2] M. Bacal, *Physica Scripta* T2/2 (1982) 467.
- [3] E. Surrey, in *Injector Tests for the Positive/Negative Ion Beamline for the TESLA Accelerator Installation*, AEA Technology report 41971/D5 A.
- [4] C. Lejeune and J. Aubert, *Advances in Electronics and Electron Physics, Suppl.* 13 A (1979) 159.